Bioresource Technology 441 (2026) 133522

Contents lists available at ScienceDirect

Bioresource Technology

journal homepage: www.elsevier.com/locate/biortech

Evaluation of calcium alginate beads immobilization of Chlorella vulgaris for biomass production in space life support systems

Francesca Mazzolini [a,*], Eva Carraro [a], Donatella Peressini [b], Micol Bellucci [c], Graziano Tassinato [d], Cristina Cavinato [a]

[a] Ca' Foscari University of Venice, Department of Environmental Sciences, Informatics and Statistics, via Torino 155, Venezia 30172, Italy
[b] University of Udine, Department of Agricultural, Food, Environmental, and Animal Sciences, Via Sondrio 2/A, Udine 33100, Italy
[c] Agenzia Spaziale Italiana (ASI), Via del Politecnico snc, Rome 00133, Italy
[d] Green Propulsion Laboratory, VERITAS spa, via della Geologia 31, Fusina 30176, Italy

HIGHLIGHTS

- *C.vulgaris* successfully grow in alginate beads for space-oriented cultivation.
- A bead-to-volume ratio (1:1) lead to a biomass productivity of 0.240 g/(L·d).
- Protein 18–24%, lipids 27–32%, and carbohydrates 11–12% on DW basis.
- Simple harvesting, reducing energy and resource demand.

GRAPHICAL ABSTRACT

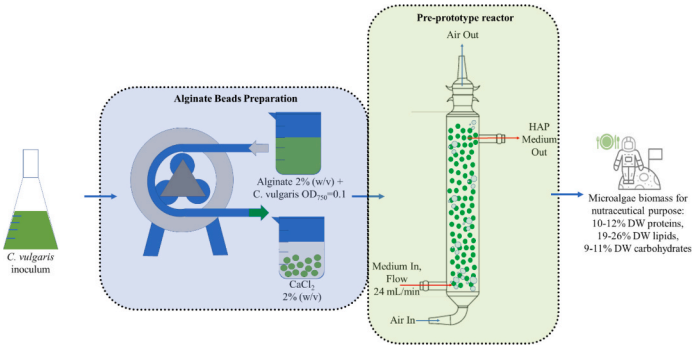

ARTICLE INFO

Keywords:
Entrapment
Microalgae
Space-base

ABSTRACT

As space missions extend in duration and distance, there is an increasing need for autonomous life-support systems capable of recycling resources and producing essential compounds *in situ.* In this context, alginate-entrapped microalgae were used to assess growth under reduced liquid conditions, testing two different beads-to-volume ratios (1:1 and 1:2). In batch cultures conducted in flasks without aeration, the immobilized microalgae using HEPES-Acetate-Phosphate (HAP) medium reached a maximum dry weight (DW) of 0.93 ± 0.03 g/L and 33.65 ± 1.19 x 10^6 cells/mL in the 1:2 configuration, compared to 1.01 ± 0.02 g/L and 37.44 ± 1.56 x 10^6 cells/mL in suspension. Biomass productivity peaked at 404 mg/(L·d) for suspension and 240 mg/(L·d) for 1:2 immobilized cultures. Biochemical analysis of immobilized biomass revealed high nutritional value, with up to 32.5 % DW lipids, 23.6 % DW proteins, and 12.5 % DW carbohydrates. In the pre-prototype column reactor with medium recirculation and air bubbling, microalgae showed lower productivity than in batch tests indicating the need for further optimization of process configuration. Immobilized *Chlorella vulgaris* offers a trade-off between reduced productivity and engineering advantages, such as ease of recovery,

* Corresponding author at: via Torino, 155, Venezia, 30172, Italy (F. Mazzolini).
E-mail addresses: francesca.mazzolini@unive.it (F. Mazzolini), eva.carraro@unive.it (E. Carraro), donatella.peressini@uniud.it (D. Peressini), micol.bellucci@asi.it (M. Bellucci), g.tassinato@gruppoveritas.it (G. Tassinato), cavinato@unive.it (C. Cavinato).

https://doi.org/10.1016/j.biortech.2025.133522
Received 7 August 2025; Received in revised form 9 October 2025; Accepted 15 October 2025
Available online 20 October 2025

and suitability for automated, closed-loop bioregenerative in space life-support systems as well as for terrestrial application.

1. Introduction

Scientific and technological progress has enabled humanity to consider longer and more complex space missions (Smith et al., 2022). However, the major constraint of space exploration is the need to maintain an Earth-based resupply missions for essential resources such as food, oxygen, and water, as well as for waste management (Klopotic et al., 2023). This dependency significantly increases mission costs and imposes a distance limit on exploration. Notably, the cost of transporting materials to space remains over $10,000 per kg (Volpin et al., 2020). To reduce this dependence, researchers are advancing Life Support Systems (LSS) capable of sustaining human life *in-situ*. Bioregenerative life support systems (BLSS) aim to create a closed-loop environment in which plant-growing modules, microbial bioreactors, and advanced environmental control systems regenerate essential resources, such as oxygen, water, and food (De Micco et al., 2023). Different projects (e.g. MELISSA, PBR@LSR, BIOS-I, and BIOS-III) have focused on these systems through Earth-based simulations and experiments on the International Space Station (ISS), but the development of efficient and reliable BLSS remains a key challenge (Santomartino et al., 2023, Fahrion et al. 2021).

In this context, microalgae have emerged as a promising component for BLSS due to their ability to efficiently convert CO_2 into oxygen, recycle nutrients, and provide nutrient-rich biomass. Recent work by Revellame et al. (2024) demonstrates that microalgae can outperform higher plants in BLSS for biomass yield, illumination, water demand, and can grow even on waste streams. *Chlorella* spp., in particular, are attractive because of their robust growth, high photosynthetic efficiency, and nutritional value, including proteins (40–60 % of dry weight), lipids (5–20 %, rich in polyunsaturated and omega-3), carbohydrates, vitamins (A, B-complex, C, E) and minerals (Ca, Mg, K, Zn) (Canelli et al., 2021; Mendes et al., 2024). Studies have also shown their adaptability to microgravity and spaceflight environments, reinforcing their relevance for future missions (Santomartino et al., 2023; Wang et al., 2024; Cycil et al., 2021). However, conventional suspended cultivation methods remain resource-intensive, requiring large amounts of water and nutrients, and involve a complex, high-cost harvesting process, that can account for 20–30 % of total production costs (Moreno-Garrido, 2008; Han et al., 2023). Bioreactor design optimization, as demonstrated by Fahrion et al. (2021), is essential to address gas–liquid exchange and light penetration limitations in space-based algal cultivation. Microalgae immobilization offers an alternative approach that can enhance biomass recovery and stability, while potentially reducing the need for complex mixing and harvesting systems (Hu et al., 2021).

Immobilization can be classified into two main categories: i) passive, as biofilm-based, and ii) active, as with polymer matrix (Moreno-Garrido, 2008). For this last method, various immobilization matrices have been explored, including: i) polysaccharide gels (such as alginates, agar, carrageenan, chitosan and poly galacturonic acid), and ii) polymeric materials (such as gelatin, collagen, and polyvinyl alcohol) (Han et al., 2023). Among these, alginate-based matrices have been widely studied due to their mild gelation process, cost-effectiveness, transparency, and high biocompatibility (Bauer et al., 2020; Han et al., 2023). Alginate, derived from brown algae, is an unbranched binary copolymer of 1–4 linked β-D-mannuronic acid (M) and α-L-guluronic acid (G) (Bauer et al., 2020; Gomez et al., 2009). The varying proportion of G-G blocks, G-M blocks, and M−M blocks determine the polymer's physiochemical properties (Han et al., 2023). Bivalent ions, such as Ca^{2+}, are commonly used to crosslink alginate by binding to its guluronic acid blocks, forming a stable "egg-box" structure. This mild gelation process occurs at room temperature, minimizing stress on microalgae cells (Cao et al., 2020). Liu et al. (2024) have shown that novel hydrogel scaffold designs can increase yield per water unit by nearly 9-fold in microalgae cultures, addressing one of the key resource constraints. Despite these advantages, immobilization techniques still face important challenges, including mass transfer limitations, bead stability and reusability, cell leakage, and light penetration (Bauer et al., 2020; Han et al., 2023). Most immobilization studies have focused on wastewater treatment, while few have investigated its potential for biomass growth and bioactive compounds production (Bauer et al., 2020; Han et al., 2023).

Despite its potential, limited research has optimized immobilized microalgae cultures for enhanced growth and biomass productivity for space life support. In particular there is limited knowledge of how immobilization in alginate matrix influence growth dynamics, biomass yield and biochemical composition of microalgae. To address this gap, in this study, we present a novel approach by cultivating *Chlorella vulgaris* immobilized in calcium alginate beads under mixotrophic conditions. Unlike most immobilization studies that employ photoautotrophic metabolism and suspended culture for space application, we deliberately used another type of microalgae metabolism and a reduced liquid volume, mimicking the resource constraints of BLSS and aiming to minimize water use while facilitating downstream harvesting more easily separated compared to suspended cultures, reducing the need for energy-intensive harvesting processes. Furthermore, we assessed not only bead morphology and cell viability but also growth parameters, biomass yield, and biochemical composition, starting from controlled batch flask to a pre-prototype photobioreactor system. By integrating mixotrophic metabolism with immobilization in a resource-efficient setup, our work provides new insights into optimizing microalgal productivity for closed-loop space life support systems.

2. Materials & methods

2.1. Microorganism and culture medium

The axenic culture of microalgae *Chlorella vulgaris NIES-224* was obtained from the culture collection of INRAE-LBE (Narbonne, France) on an agar plate in a HEPES-Acetate-Phosphate (HAP) medium. The culture was maintained on this synthetic medium following the method described by (Lacroux et al., 2021).

The pre-culture was maintained in an orbital shaker (150 rpm), under constant illumination provided by a 4000 K white LED at 80 μmol/(m^2·s). The temperature was controlled at 30 °C in a thermostatic chamber (Pol-Eko, Poland). After the 4 days of cultivation, during the exponential growth phase, algal cells were harvested by centrifugation at 3900 rpm for 5 min. The pellet was washed and resuspended in sterile deionized water, resulting in a concentrated algal suspension to use for inoculating the tests.

All chemicals were purchased from Sigma Aldrich (USA).

2.2. Microalgae immobilization on alginate beads

The microalgae *C. vulgaris* was immobilized in alginate beads using the ionotropic gelation method, where $CaCl_2$ was used as a cross-linker (Naskar et al., 2024). The procedure described by (Cao et al., 2020) was followed with some modifications, namely changes in crosslinking time and microalgae concentration.

Sodium alginate was dissolved in the medium at pH 7 to prepare a 2 % (w/v) solution. A 1.5 mL aliquot of algal suspension was mixed with the alginate solution to obtain a final $OD_{750} = 0.1$ and an inoculum-to-medium ratio of 10 μL/mL. The resulting solution was dropped into a 2 % (w/v) $CaCl_2$ solution to form Ca-alginate beads (~5 mm diameter)

using a peristaltic pump (flow rate: 24 mL/min). After 1 h of crosslinking reaction, the beads were thoroughly washed with distilled water and then used for the tests. All procedures were performed under sterile conditions in a laminar flow hood. The same procedure was repeated to obtain an alginate solution with distilled water as control. The different immobilization configurations and the respective labels are reported in Table 1.

2.3. Analysis for beads characterization

2.3.1. Morphology characterization

The microalgae-immobilized alginate beads were analysed for morphological and dimensional characteristics using the open-source software ImageJ®. Digital images of the beads were captured against a contrasting background, with a ruler included for calibration, using a digital camera (Aguirre Calvo and Santagapita, 2016; Ciarleglio et al., 2023). Circularity, roundness, solidity and aspect ratio (AR) were determined as indicators of particle roundness (Vetrano et al., 2023). Feret's diameter (or maximum caliper length) that is the longest distance between two parallel tangents on opposite sides of an object, were also determined. If the object is a circle, the Feret's diameter is equal to the diameter of the circle. These main parameters were analyzed for at least 10 beads.

In addition, scanning electron microscopy (SEM – Hitachi TM 3000 Tabletop), was performed on freeze-dried beads to investigate the surface morphology, as well as the medium and microalgae distribution throughout the bead matrix. Beads were fixed to the SEM holder using double-sided adhesive tape and coated with a thin metal layer. Measurements were conducted at different magnification and at an acceleration voltage of 15.00 kV.

2.3.2. Water content and swelling behaviour

The total water content (WC, %) of the beads was determined gravimetrically as reported by (Zazzali et al., 2019). The swelling behaviour was calculated as reported by Vetrano et al. (2023) with some modifications: the alginate beads were immersed in the growth medium and kept on an orbital shaker (150 rpm). All the measurement was performed on ten beads.

2.3.3. Diffusion preliminary assessment using bromothymol blue

The diffusion of small molecules and nutrients from the medium in alginate beads matrix was preliminary evaluated using the pH indicator bromothymol blue. Beads were prepared by dissolving 2 % (w/v) alginate in distilled water with the addition of bromothymol blue and dropped in a $CaCl_2$ (2 % (w/v)) solution. The prepared beads were immersed in a NaOH (pH 10) and in a HCl (pH 3) solutions. The diffusion rate was assessed by measuring the time required to detect the colour change in the pH-indicator inside the alginate matrix and reach equilibrium.

Table 1
Description of tests labels used in this study.

Test ID	Reactor type	Beads-to-medium volume ratio
HAP-MA-1:1	Flask	1:1
HAP-MA-1:2	Flask	1:2
C-HAP-MA-1:1	Pre-prototype column reactor with recirculation and aeration.	1:1
C-HAP-MA-1:2	Pre-prototype column reactor with recirculation and aeration.	1:2
Bead ID	**Medium**	**Microalgae**
AB-H2O	Distilled water	No
AB-H2O-MA	Distilled water	Yes
AB-HAP	HAP medium	No
AB-HAP-MA	HAP medium	Yes

2.3.4. Mechanical properties

The mechanical strength was evaluated by a compression test at 25 °C according to the methodology adopted from de Jesus et al. (2019) with some modifications (TA.XT Plus Unit Texture Analyzer, Stable Micro System Ltd., Godalming, UK). The distance between the probe (P/36R cylinder probe, diameter 36 mm) and the flat plate was adjusted to 10 mm. The force (N) at 50 % compression was used as an index of the specimen resistance or hardness. Each sample was tested with 10 replicates.

2.4. Culture conditions of immobilized Chlorella vulgaris

Immobilized microalgae were batch-cultured in 300 mL flasks with a working volume of 150 mL using HAP as the growth medium for mixotrophic metabolism (HAP-MA-1:1 and HAP-MA-1:2). Two different volumetric beads-to-medium ratios (1:1 and 1:2) were tested for 7 days with periodic sampling under reduced free liquid volume conditions for potential use in space applications. Algae beads were kept in suspension using an orbital shaker set at 150 rpm. Batch cultures in suspension mode served as controls. The culture conditions for all the tests were the same as those used for inoculum preparation. If necessary, the pH was adjusted to 7 using an 1 M HCl solution. All the tests were performed in triplicate. Beads were observed under optical microscopy at each sampling from their cross-section. At the end of the test, microalgae biomass was recovered for further analysis (biomass composition).

2.5. Pre-prototype culture conditions of immobilized Chlorella vulgaris

The same culture conditions used for the batch tests were applied in a pre-prototype column reactor (Fig. 1) with medium recirculation (24 mL/min) and air bubbling from the bottom through a sintered glass filter (160–250 μm of porosity). Air bubbling was used to ensure proper mixing of the medium and beads inside the reactor. The pre-prototype reactor was made of transparent glass with a height of about 30 cm and external diameter of 5 cm. Growth and nutrient consumption were monitored over 7-days test period with daily sampling. The tests were labelled as C-HAP-MA-1:1 and C-HAP-MA-1:2.

2.6. Analysis of growth parameters

Microalgae growth in immobilized culture was quantified by measuring the optical density at 750 nm (OD_{750}) using a UV–Vis spectrophotometer (ONDA Spectrophotometer UV–vis 31 Scan). The wavelength of 750 nm was chosen to minimize pigment interference (Griffiths et al., 2011). Before measurements, the microalgae beads were dissolved in a 0.5 M trisodium citrate ($Na_3C_6H_5O_7$) solution (Murujew et al., 2021). Algae beads (1 g, ≈13 beads) were added to 4 mL of the citrate solution and stirred for 20–30 min. As a blank, alginate beads without microalgae were used. To determine the dry weight (DW, g/L) and cell count (CC, $x10^6$ cells/mL) were used the calibration curves from the suspended biomass test. Dry weight and biomass productivity (Pb, mg/(L·d)) was determined as reported by (Fuad et al., 2021).

Microalgae cell density was determined as reported by (Pastore et al., 2018). All the measurements were done in duplicate 1–2 times per day, depending on the growth phase. The correlation equations were:

$$DW = 0.2701 \times OD_{750}, R^2 = 0.997 \quad (1)$$

$$CC = 9.7638 \times OD_{750}, R^2 = 0.994 \quad (2)$$

2.6.1. Nutrients in the cultivation media

The analysis of carbon and nitrogen source consumption was monitored in the liquid phase after filtration with a 0.22 μm cellulose acetate

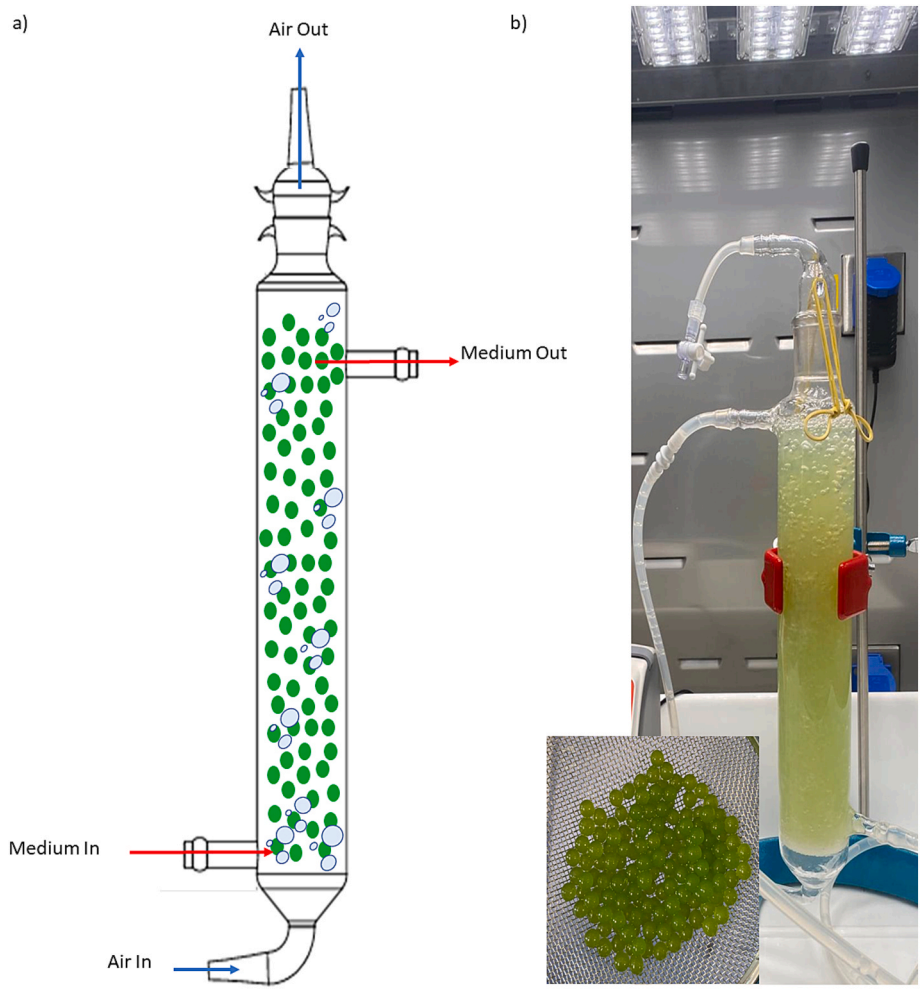

Fig. 1. A) pre-prototype column reactor scheme for microalgae alginate beads growth, and b) pre-prototype in thermostatic chamber used for the tests in lab.

filter. The remaining concentration of acetic acid in the cultivation media was measured using an HPLC (Agilent Technologies 1100 series, Santa Clara, CA, USA) column Acclaim™ Organic Acid 5 μm 4x150 mm with a mobile phase of methanesulphonic acid 2.5 mM and acetonitrile at a flow rate of 1 mL/min. The residual ammoniacal nitrogen was measured using an ion selective electrode-ISE (HI4101, HANNA Instruments-USA) with a PTFE membrane permeable to NH_3 gaseous. The nutrient removal rate (NRE) was calculated by Eq. (3):

$$NRE(\%) = \frac{X_i - X_f}{X_i} \times 100 \quad (3)$$

where X_f and X_i are the concentration of acetic acid or N-NH_4^+ (mg/L) at the end and at the start of the test, respectively.

2.6.2. Biomass characterization

At the end of the test, microalgae biomass was harvested by dissolving the beads in a 0.5 M sodium citrate solution at a 1:4 ratio, followed by centrifugation at 9000 rpm for 5 min, and then lyophilized for the determination of biomass composition. Lipid content was quantified using the sulfo-phospho-vanillin method as reported by (Lacroux et al., 2021). The proteins quantification was determined using the Bradford's method and phenol–sulfuric acid for carbohydrates analysis were conducted following the methods of Andreeva et al. (2021).

2.7. Statistical analysis

Data analyses were performed using RStudio programme (version 4.4.2, R Foundation for Statistical Computing) and data were reported as means ± standard deviation (SD). Data were analysed using Student's *t*-test to determine any statistical difference. The significance was determined at the 95 % confidence level ($p < 0.05$).

3. Results & Discussion

3.1. Beads formation and crosslinking

Beads formation through the extrusion dripping method of alginate into $CaCl_2$ solution occurred due to ionotropic gelation between divalent calcium ions (Ca^{2+}) and the negative charged carboxylate group of alginate polymer (Banerjee et al., 2019). Particularly, at a pH higher than the pKa of mannuronic (3.65) and glucuronic (3.38) acids, as in the case of this study where the alginate solution had a pH of 7, the carboxylic acid groups (–COOH) are deprotonated and negatively charge (Naskar et al., 2024). As previously described alginate beads crosslink via the egg-box structure, which affect porosity and stability (Bajpai and Sharma, 2004). Crosslinking occurs rapidly at the outermost layer in direct contact with the $CaCl_2$ solution, while it proceeds more slowly in the inner layers of the bead (Hu et al., 2021). Regarding microalgae, they are physically entrapped within the polymer matrix. At neutral pH, the microalgae surface had a negative zeta potential (−18 mV) due to the presence of functional groups such as carboxylic, sulphate, phosphate, amine groups. This could result in electrostatic repulsion between microalgae and the negative charged functional groups of the alginate polymer (Procházková et al., 2012). The structural stability and the

physical entrapment of microalgae through the matrix is particularly relevant for BLSS application, where beads integrity and stability are crucial to optimize the system performance. For this reason, the initial part of this study focused primarily on determining the most important characteristics of alginate beads.

3.2. Beads characterization

Alginate beads (AB-HAP-MA) were analysed through image software both after their production by the extrusion dripping method (0 h), and again after 67 and 163 h of testing. As control, the samples AB-HAP, AB-H_2O, and AB-H_2O-MA, were analysed. The size and morphological characterization of the beads are crucial as they can influence physico-chemical properties, such as nutrient exchange for microalgae growth (Aguirre Calvo and Santagapita, 2016). Evaluating the sphericity of alginate beads is a key parameter for ensuring their long-term stability, especially for their use in long-term space missions. In fact, Lee et al. (2013) reported that non-spherical beads exhibit reduced gel strength and stability compared to spherical ones. The data of the different analysed parameters by digital image processing techniques have been reported in Table 2.

No significant difference ($p > 0.05$) was observed independently of microalgae presence or medium used for the parameters of circularity, roundness, solidity and aspect ratio (AR) and Feret diameter. This indicates that the alginate beads maintain their nearly spherical shape, with values of these parameters close to 1. Similarly, in the study by (de Jesus et al., 2019), the entrapment of microalgae did not affect the spherical shape of the beads. Maintaining sphericity ensures predictable nutrient diffusion and uniform growth of microalgae, an advantage for scale-up in reactors. Spherical bead formation depends on several factors like alginate viscosity, surface tension, tip size, and dripping distance, which affect droplet stability (Ciarleglio et al., 2023). Masoomi Dezfooli et al. (2022) reported that a 2 % (w/v) alginate solution at 26 °C has a viscosity of 930 mPa·s, aligning with the experimental conditions of this study of a 2 % (w/v) alginate solution at 25 °C and a 9 cm dripping height, which yielded stable spherical beads. The dripping height used in this study fits within the effective range of 3–270 cm identified by (Lee et al., 2013) for medium-viscosity alginate. The use of experimental conditions that allow obtaining beads with a spherical geometry, such as those adopted in this study, allows for an improvement in the stability of the spheres and better handling. For microalgae immobilization, bead morphology, as size, influences also nutrient and gas diffusion (De Jesus et al., 2019). In this study, was use "macrobeads" with a reproducible diameter of 5 mm to facilitate an easy harvesting and handling, serving as a compromise despite the potential limitation in nutrient diffusion.

A further morphological analysis regarded the acquisition of SEM images to examine both the external surface morphology (500x magnification) and to highlight the immobilization of microalgae within the polymer matrix (1.8Kx magnification). As shown in Fig. 2b, the lower magnification images reveal the overall structure of the beads with the salts medium distribution. Contrarily, the Fig. 2a shows the smooth surface of the alginate beads produced without growth medium using distilled water. The homogeneous distribution of salts throughout the polymer matrix is essential for the sustenance of microalgal growth within the matrix. Successful physical encapsulation of microalgae is evident in the higher magnification image (Fig. 2c) where the alginate network forms a 3-D scaffolds that entraps and spatially distributes the microalgae through the matrix.

The water content (WC) in the bead is influenced by the syneresis process during the formation of the alginate gel network and the water exchange across the bead boundaries due to osmotic effects (Zazzali et al., 2019). Understanding the WC in alginate beads and the role of the medium used in their preparation is essential, considering the significant impact of water on beads stability, and on the mass transfer capacity due to the porosity and tortuosity (Aguirre Calvo and Santagapita, 2016; Kashima and Imai, 2017; Yoshida and Kashima, 2025). The WC content was tested after their preparation in four different samples using water or growth medium in the alginate solution and with or without microalgae. No significant difference ($p > 0.05$) were observed among the samples, with all the beads exhibiting a water content of around 95 %, indicating a higher water content. The obtained value is slightly lower than those reported by Ciarleglio et al. (2023) and Aguirre Calvo and Santagapita (2016) in a range between 96 and 98 % using similar experimental conditions of alginate, $CaCl_2$ concentration and temperature. So, the low WC% content suggest a tighter structure probably due to high guluronic content into alginate polymer used (Kashima and Imai, 2012). This network has low porosity but high tortuosity thus mass transfer could be slower (Yoshida et al., 2025). The moderate swelling ratio of 55–65 % is consistent with this interpretation: although the beads are highly hydrated, the tighter network limits additional water uptake. The alginate beads containing HAP medium without microalgae exhibit higher swelling ratio (SR%) of 65 %. This result is consistent with the medium composition, as this mechanism is pH and Na^+ dependent as explained by (Malektaj et al., 2023) and (Matyash et al., 2014). Interestingly, HAP beads loaded with microalgae have a significantly lower swelling degree (56 %) than those without microalgae ($p < 0.05$, *t*-test), with values similar to those of beads prepared using water (55 %). The lower degree in water-prepared beads may be attributed to the absence of Na^+ in the preparation solution (Bajpai and Sharma, 2004). The compressive resistance measurements, of approximately 1.04 ± 0.05 N showed no significant differences ($p > 0.05$) among beads prepared with water or growth medium. The physical properties of alginate beads are largely affected by characteristics such as molar mass, G/M blocks ratio, polymer concentration, and the type and concentration of the cross-linking agent (de Jesus et al., 2019). In the study by de Jesus et al. (2019), the mechanical properties of alginate beads obtained under similar condition (2)% (w/v)) of alginate and 2 % (w/v) $CaCl_2$ were also tested, comparing the strength of the beads with and without microalgae. As in this study, they found no significant difference with the addition of microalgae to the polymer matrix. The mechanical property was examined considering potential applications in a space environment, particularly in a column reactor for the production astronaut's nutraceutical diet addition. This is important because it indicates the susceptibility of the beads to different environments, transportation in fluids, and exposure to shear or normal forces (Zazzali et al., 2019).

Table 2
Different morphological parameters analysed by digital image processing.

Sample	Time (h)	Circularity	Roundness	Solidity	AR	Feret
AB-HAP	0	0.90 ± 0.01	0.95 ± 0.02	0.97 ± 0.01	1.05 ± 0.02	0.49 ± 0.02
AB-H_2O		0.90 ± 0.01	0.94 ± 0.02	0.97 ± 0.01	1.06 ± 0.02	0.49 ± 0.02
AB-HAP-MA		0.90 ± 0.02	0.95 ± 0.04	0.96 ± 0.02	1.05 ± 0.04	0.52 ± 0.02
AB-H_2O-MA		0.89 ± 0.02	0.94 ± 0.03	0.98 ± 0.01	1.07 ± 0.04	0.51 0.01
AB-HAP-MA	67	0.86 ± 0.05	0.96 ± 0.02	0.97 ± 0.02	1.04 ± 0.02	0.51 ± 0.03
AB-HAP-MA	163	0.89 ± 0.02	0.97 ± 0.01	0.98 ± 0.01	1.04 ± 0.02	0.51 ± 0.02

*__AB-HAP-MA__: alginate beads produced using microalgae growth medium with entrapped microalgae; __AB-HAP__: alginate beads produced using microalgae growth medium without microalgae; __AB-H_2O-MA__: alginate beads produced using water with entrapped microalgae; __AB-H_2O__: alginate beads produced using water without microalgae; each point average (n = 10).

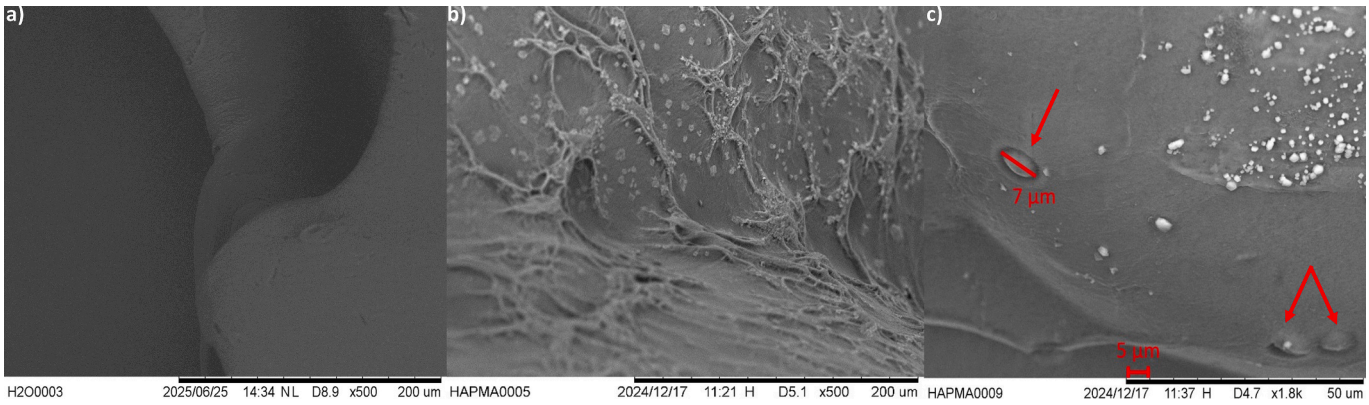

Fig. 2. A) 500x magnification surface structure of alginate bead without growth medium, b) with growth medium and c) microalgae encapsulation into the alginate matrix.

The effective diffusion coefficient (D_{HAeff}) was estimated using the approach reported in (Baldo et al., 2024; Souza et al., 2024) which is based on the use of a platinum microelectrode and by chronoamperometry as discussed in details (see supplementary materials). The best fitting of experimental values and the theoretical equation provided D_{HAeff} = 2.4 x10^{-10} m^2/s. This value was also confirmed by using steady-state voltammetry (Baldo et al., 2024) and the limiting current (I_l) given by the following equation:

$$I_l = 4nFrD_{HAeff}C_{HA} \quad (4)$$

where n is the number of electrons involved, F is the Faraday constant, r is the radius of microelctrode, D_{HAeff} and C_{HA} are the diffusion coefficients and concentrations of acetic acid species, respectively. The experimental limiting current provided I_l = 4.52 x 10^{-9} A provided 2.3x10^{-10} m^2/s, which compares well with that obtained by chronoamperometry. In addition, D_{HAeff} found here also compare with those reported in the literature for similar sized molecules in alginate gels (e.g. urea) (Kashima and Imai, 2012). However, the value found in alginate for acetic acid is lower than that reported in water solution (0.95 x 10^{-8} m^2/s) (Baldo et al., 2024). This reduction can be attributed to the relatively tight polymer network, smaller pores, increasing tortuosity and obstruction that decrease mobility of the species. The diffusion properties of alginate beads were evaluated also using the pH indicator bromothymol blue to assess the transport of acetic acid through of the matrix. Bromothymol blue, a pH-sensitive dye, exhibits a colour shift based on the pH environment (Rungsima et al., 2021). Moreover, unlike other dyes, is a low molecular weight molecule (624 Da) and is uncharged, so its diffusion is not influenced by any interactions with the charged groups present in the alginate structure, making it a suitable indicator for visualizing diffusion (Fig. 3) within the beads (Neves et al., 2024).The beads, immersed at first in a solution (KOH 3 M, pH 10) and then in an acidic solution (Acetic acid 20 mM, pH 3.78), were observed over time (Fig. 3a). The colour change at a specific time reflects how far CH_3COOH diffuses through the polymer matrix.

The colour shift of a cross-section was analysed at ImageJ program after 30 min to estimate the radius of acetic acid penetration during time and compare with the electrochemical data for a further confirmation (Fig. 3b). The colour-front analysis revealed that after 30 min the acetic acid was diffused throught the matrix at 1.06 ± 0.08 mm confirmed by the theoretical estimation using D_{HAeff} (≈1.2 mm). The permeation process is influenced by factors such as bead porosity, crosslinking density, and the presence of other components that may alter the internal structure of the hydrogel network. A faster diffusion rate suggests a more open structure with lower crosslinking, whereas slower diffusion indicates a denser network with restricted molecular mobility (Privman et al., 2016). Understanding the diffusion behaviour of alginate beads is essential for optimizing their applications in bioreactors, and other biotechnological processes. In this study, the pH of the alginate solution for microalgae growth was set to 7, which is higher than the pKa values of the two monomers of the alginate polymer chains. At this pH, the –COOH functional groups are in their anionic form ($–COO^-$), enabling them to attract positively charged species such as NH_4^+, thereby facilitating their absorption into the matrix. Conversely, phosphate ions (PO_4^{3-}) can interact with the Ca^{2+} ions (Banerjee et al., 2019). Considering the importance of nitrogen for microalgal growth, the diffusion coefficient of this nutrient in the form of NH_4^+ was also estimated using bulk-uptake measurements and modelling based on fitting the diffusion series equation as discussed in details (see supplementary materials). The effective diffusion coefficient of ammonium (D_{NH4eff}) in the alginate matrix was estimated to be approximately (1.2 ± 0.78) x10^{-10} m^2/s,

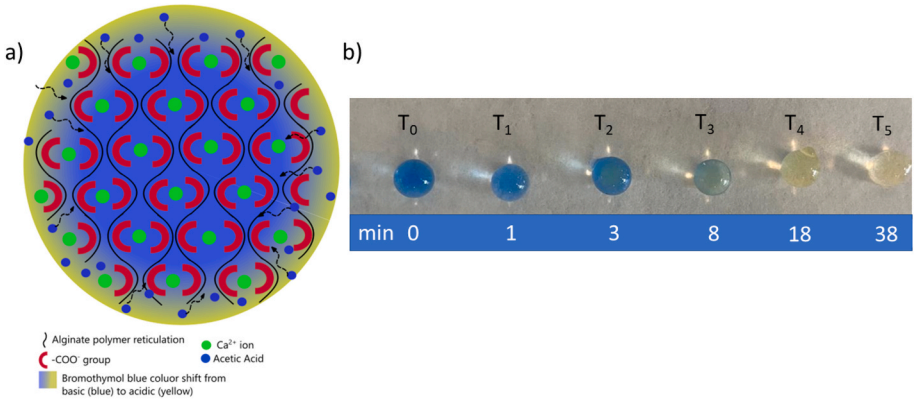

Fig. 3. A) scheme of diffusion through alginate beads, and b) alginate beads colour change at different sampling time.

which is similarly about one order of magnitude lower than its value in aqueous solution (Stefan-Kharicha et al., 2018). This result also indicates that diffusion of ammonium is hindered within the alginate network, consistent with the observations for acetic acid.

Therefore, from the perspective of immobilized microalgae growth in a BLSS system, it is an interesting result for long-term applications that microalgae are able to grow in the matrix even when nutrient diffusion coefficients for compounds such as acetic acid and nitrogen are lower than in aqueous solution, and that the addition of microalgae does not compromise the matrix stability during the growth period.

3.3. Growth of immobilized microalgae Chlorella vulgaris

The growth profile of *Chlorella vulgaris* was analysed under suspended (as control) and immobilized conditions over 160 h (Fig. 4). The increase in OD_{750} confirms active photosynthesis, as explained by previous studies (Banerjee et al., 2019; Tam & Wong, 2000). In contrast to suspended biomass, the HAP-MA-1:1 and HAP-MA-1:2 immobilized cultures did not exhibit an initial lag phase consistent with literature for similar systems (de Barcellos et al., 2024).

The suspended culture reached the highest growth (OD_{750} = 3.6) within 72 h before entering the stationary phase. In contrast, immobilized cultures grew more slowly with the 1:2 beads-to-volume condition achieving a higher OD_{750} (2.7) than the 1:1 condition (2.2) at 160 h. The immobilized microalgae demonstrated continuous growth even after the initial exponential phase, likely due to progressive colony expansion within the alginate matrix (Fig. 5).

The reduced growth in the 1:1 condition could be attributed to self-shading and insufficient aeration among beads, as previously reported by Tam and Wong (2000). Cross-section analysis of the beads revealed single cell at the start (green arrows) after their inoculation, followed by colony formation over time (red and blue arrows). Consistently with previous studies (Moreno-Garrido, 2008) as colonies densify from 72 to 157 h, nutrient diffusion and light penetration gradually became limiting, explaining slower overall productivity relative to suspension cultures. In particular, the difference from the suspension culture could be attributed to the lower diffusion coefficients of acetic acid and ammonium within the alginate matrix. Nonetheless, the uniform distribution of the microalgae colonies suggests that there is a homogeneous diffusion of nutrient and light through the beads.

This growth pattern highlights both the advantages and limitation of immobilization. On one hand, the efficacy of the immobilization system

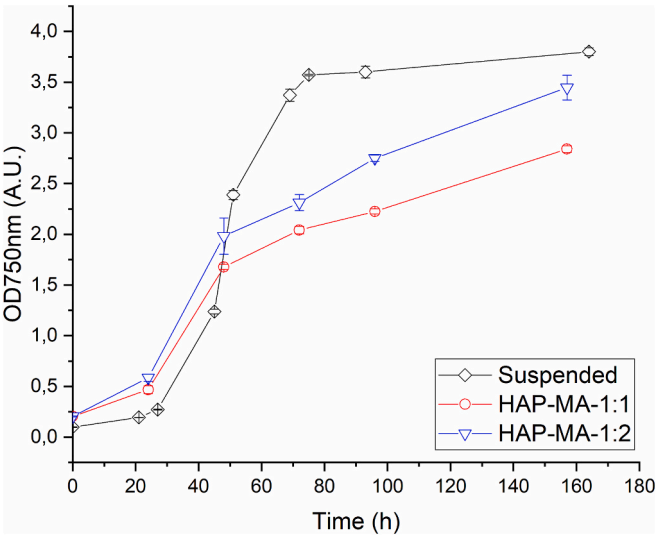

Fig. 4. Growth curve of microalgae immobilized in alginate beads at two different beads-to-volume ratios (1:1 and 1:2, n = 3), and suspended biomass growth curve as control (n = 3).

on microalgae growth. On the other hand, as colonies become denser, diffusion of nutrients and light penetration are progressively limited, which may explain the slower overall productivity compared to suspended cultures. Optimizing bead size, porosity, and reactor hydrodynamics could mitigate these diffusion constraints while retaining the harvesting benefits of immobilization.

Biomass accumulation, expressed as dry weight (DW) and cell concentration (CC) (Table 3), mirrored this trend, confirming that lower bead density enhances light penetration and nutrient diffusion, promoting higher productivity.

Although growth and productivity were lower than in suspended cultures, immobilization offers operational advantages such as simplified harvesting and enhanced culture stability. This trade-off is particularly relevant for BLSS, where efficient resource recovery may outweigh the maximization of short-term productivity. The specific growth rate (μ) of immobilized cultures were lower (1.0–1.1 d^{-1}) than that of suspended biomass (1.7 d^{-1}), representing a ≈35 % reduction in growth kinetics due to immobilization. This result is consistent with previous observations for other green microalgae species (Benasla and Hausler, 2018). Productivity followed the same trend: suspended > HAP-MA-1:2 > HAP-MA-1:1, confirming that lower bead density mitigates diffusion and shading limitations. In particular, our mixotrophic immobilized system achieved productivity comparable to photoautotrophic immobilized cultures reported in literature (0.19–0.25 g/(L·d)), highlighting the suitability of mixotrophy under resource-limited conditions relevant to space habitats (Benasla and Hausler, 2018; Moreno-Garrido, 2008).

While most studies on immobilization focus on photoautotrophic growth, our mixotrophic setup achieved comparable productivity, demonstrating its potential in the suitability of this approach under resource-limited conditions representative of space habitats. Overall, while immobilization did not maximize initial productivity, it provides a more sustainable strategy by facilitating harvesting, reducing water demand, and promoting culture stability. These features make immobilized cultivation a promising candidate for integration into future BLSS, especially when long-term robustness and process simplicity are prioritized.

Lyophilized biomass harvested at the end of the test was analyzed to determine their nutritional composition (Table 4).

Protein content (18–24 % DW) was lower than values typically reported for free-living *C. vulgaris* under photoautotrophic conditions (40–60 %), likely due to partial nitrogen limitation within the bead matrix and the immobilization-induced stress. In contrast, lipid content (27–33 % DW) exceeds typical ranges (5–20 %) and may reflect stress-related lipid accumulation often observed in immobilized or nutrient-limited microalgae (Canelli et al., 2021; Mendes et al., 2024). Carbohydrate content remained within the expected range (~11–12 % DW), suggesting that energy storage was maintained despite growth constraints. The differences between HAP-MA-1:1 and HAP-MA-1:2 biomass composition emphasizes the importance of optimizing bead density for both growth and biomass composition in BLSS applications. Despite compositional variations, the immobilized biomass retained essential nutritional quality: proteins for astronaut nutrition, lipids for energy and essential fatty acids, and carbohydrates for energy storage. These findings support the integration of immobilized, mixotrophic *C. vulgaris* into space-based life support systems, where balancing productivity, nutrient density, and harvesting efficiency is crucial.

3.4. Pre-prototype culture conditions of immobilized Chlorella vulgaris

The pre-prototype column reactor was operated under the same culture conditions as the batch assays (Section 3.3), but with air bubbling (0.038 % CO_2) from the base to maintain beads in suspension and medium recirculation. The initial cell concentration inside the beads was approximately 1 x 10^6 cells/mL. As reported by Moreno-Garrido (2008), this parameter strongly influences final biomass yield in

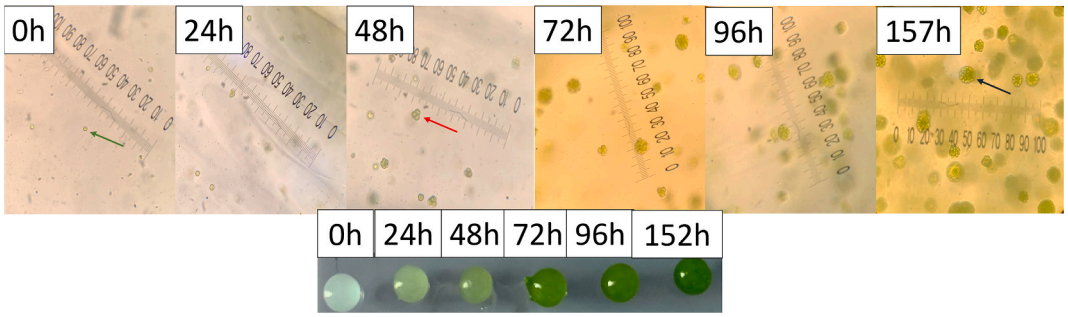

Fig. 5. Microalgae beads section over time: single colony (green arrow), growing colony (red arrow) and aggregated colony at the end of the experiment (black arrow).

Table 3
Dry weight (DW) and cell concentration (CC) at the end of the tests of immobilized microalgae, and suspended biomass, as control.

Parameters	Suspended biomass	HAP-MA-1:1	HAP-MA-1:2
DW(g/L)*	1.01 ± 0.02	0.77 ± 0.01	0.93 ± 0.03
CC (x10^6 cells/mL)*	37.44 ± 1.56	27.73 ± 0.33	33.65 ± 1.19
μ (d^{-1})	1.7 ± 0.04	1.0 ± 0.04	1.1 ± 0.03
P_b (mg/(L·d))	404 ± 0.1	199 ± 0.4	241 ± 0.2

* derived from correlation curves OD_{750}-to-DW and OD_{750}-to-CC (n = 3).

Table 4
Biomass composition of microalgae immobilized into alginate beads and grown under two different beads-to-volume ratios, 1:1 and 1:2.

	HAP-MA-1:1	HAP-MA-1:2
Proteins (% DW)	23.65 ± 2.32	18.55 ± 1.58
Lipids (% DW)	32.55 ± 8.12	27.49 ± 2.45
Carbohydrates (% DW)	11.51 ± 0.51	12.48 ± 2.10

immobilized cultures due to colony-based growth dynamics. The growth profiles in the column reactor (Fig. 6a) was like those obtained in batch tests (Section 3.3), showing no evident lag phase and rapid exponential growth, which confirms that the immobilization and bead formation process (Sections 3.1–3.2) did not harm cell viability. As observed previously (Section 3.3), the 1:1 beads-to-volume ratio resulted in slightly lower final OD_{750} than the 1:2 ratio, likely due to higher bead density causing light attenuation and nutrient limitation. A lower diffusion coefficient (Section 3.2) and higher beads-to-volume ratio magnify the growth constraints in the reactor with a different mixing mode and nutrient diffusion.

Results reported in Table 5 showed that using a column reactor with

Table 5
Culture parameters and biomass composition of the tests conducted on the pre-prototype reactor.

Parameters	C-HAP-MA-1:2	C-HAP-MA-1:1
DW(g/L)	0.200 ± 0.01	0.177 ± 0.03
CC (x10^6 cells/mL)	7.22 ± 0.33	6.40 ± 1.19
μ (d^{-1})	0.726 ± 0.01	0.732 ± 0.1
P_b (mg/(L·d))	45.49 ± 0.01	47.00 ± 0.03
Proteins (% DW)	11.74 ± 0.01	10.28 ± 0.01
Lipids (% DW)	25.96 ± 0.01	18.84 ± 0.01
Carbohydrates (% DW)	10.64 ± 0.01	9.17 ± 0.01

a higher beads density (C-HAP-1:1) reduces the microalgae biomass production due to light shading or nutrient limitation diffusion. Biomass productivity in the pre-prototype reactor (45–47 mg L^{-1} d^{-1}) was considerably lower than that achieved in flask cultures (199–241 mg L^{-1} d^{-1}). This decline is mainly attributed to light shading and diffusion constraints typical of immobilized systems. The comparison between flask test (Sections 3.3, HAP-MA-1:2 and HAP-MA-1:1) and pre-prototype test (Section 3.4, C-HAP-1:2 and C-HAP-1:1) thus highlights the scale-dependent effects of light path and hydrodynamics on immobilized microalgae growth. Future improvements in reactor geometry and internal illumination could mitigate these losses. This reduction can be also attributed to mass-transfer limitations, consistent with the tight polymer network and tortuous diffusion pathways identified in bead-characterization experiments (Section 3.2). The connection between the material properties (dense, low-porosity matrix) and reactor performance highlights the importance of tailoring bead composition and crosslinking degree for large-scale applications.

Since there is no significant difference ($p > 0.05$) between the two beads-to-volume ratios tested, and considering the need to optimize

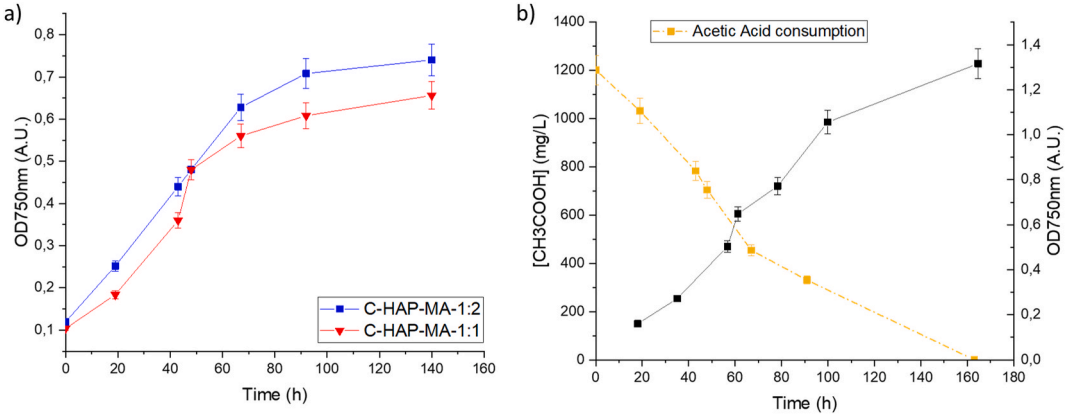

Fig. 6. A) growth curve of microalgae alginate beads at two different beads-to-volume ratios using the pre-prototype column reactor with medium recirculation (n = 2); b) Acetic acid consumption for the 1:1 sphere-to-medium ratio using water to create the alginate beads (n = 2).

resources use in a space-based environment, the 1:1 ratio was selected for the following tests.

Additionally, with the same objective in mind, it was decided to test the beads made with alginate dispersed into distilled water instead of growth medium. As shown in Fig. 6b, growth was higher in this case likely due to an ionic competition from the medium components during the bead formation process. This observation aligns with the physicochemical results from Section 3.1, where ionic components in the growth medium (notably phosphate) were shown to interact with Ca^{2+} ions, forming calcium phosphate precipitates that alter bead porosity. Such ionic interference likely reduced crosslinking homogeneity and hindered nutrient diffusion, supporting the improved performance of water-based beads (Banerjee et al., 2019).

In Fig. 6b is also reported the consumption over the time of the carbon source as acetic acid. From the graph, it is evident that the highest rate of acetic acid consumption occurred during the exponential phase of the growth curve, indicating active metabolization of the organic carbon source by microalgae (Lacroux et al., 2021). At the end of the test, after 163 h, the acetic acid was completely used, corresponding to a removal efficiency of 100 %. In beads made using medium containing acetate, external acetate levels remained unchanged, suggesting that cells primarily utilized acetate trapped within the matrix. The amount of acetate available in a 350 mL volume at a concentration of 1.2 g/L corresponds to 0.42 g. In the case of beads produced using medium containing acetate, the total biomass produced (0.172 g) is consistent with the theoretical yield based on the acetate present within the beads. This behaviour confirms the limited mass transfer across the bead boundary described in Section 3.2 and demonstrates how internal nutrient availability can support growth under immobilized conditions.

Regarding ammonium removal efficiencies (79–85 %) were comparable across all conditions (no significant differences, $p > 0.05$) confirming that immobilization did not significantly affect nitrogen assimilation. However, the reduced protein content in the biomass (Table 6) suggests localized nitrogen limitation inside the beads. This phenomenon, also discussed in Section 3.3, likely drives the observed lipid accumulation (19–26 % DW) due to nitrogen starvation, consistent with Canelli et al. (2021).

The biochemical composition of *C. vulgaris* immobilized in alginate beads matrix, cultivated in the pre-prototype column reactor and reported in Table 6 showed no significant difference between the two conditions tested of beads-to-volume ratio.

As reported by literature (Canelli et al., 2021; Spínola et al., 2023), the protein content obtained in this study was lower than those obtained in literature that is in a range of 14–65 % depending on cultivation conditions. Reduced protein levels may limit the use of immobilized biomass as a primary protein source in astronaut diets. At the same time, lipids content was higher than those reported in the literature (5–20 %). The higher lipid fraction enhances the energy density and may provide essential fatty acids critical for human health in closed habitats. Probably, the lower protein content and the higher lipids content is related to a local nitrogen starvation due to the microalgae immobilization into the alginate matrix. The carbohydrate content is within the expected range in a level that are typical for C. vulgaris and contribute to its energy content. Based on biochemical composition (11 % protein, 19 % lipids, 10 % carbohydrates, DW basis), the estimated energy value of the biomass is ~ 255 kcal/100 g DW. At the end, the results from Sections 3.3 and 3.4 demonstrate that immobilization in alginate beads maintains robust metabolic activity across scales, but also shifts macronutrient allocation toward lipid accumulation due to localized nitrogen gradients. These findings suggest that while immobilization facilitates handling and harvesting, it also alters biomass composition in ways that must be considered for nutritional planning in BLSS. Future optimization of bead formulation, aeration, and nutrient delivery could help rebalance protein and lipid levels to better meet both life-support and dietary requirements.

4. Conclusions

This study shows that *Chlorella vulgaris* immobilized in calcium alginate beads can be effectively cultivated under controlled conditions, making it suitable for bioregenerative life support systems. Although immobilization reduces productivity compared to suspension cultures, it offers advantages such as structural stability, easy biomass recovery, lower contamination risk, reduced free-liquid volume, and compatibility with automation. Bead preparation using distilled water instead of growth medium further decreases resource demand. These features support the development of sustainable closed-loop systems for space habitats. Future research should address long-term cultivation stability, reactor integration, and validation under space-analog conditions.

CRediT authorship contribution statement

Francesca Mazzolini: Writing – review & editing, Writing – original draft, Investigation, Formal analysis, Data curation, Conceptualization. **Eva Carraro:** Writing – original draft, Investigation, Data curation. **Donatella Peressini:** Writing – review & editing, Supervision, Investigation. **Micol Bellucci:** Writing – review & editing, Supervision. **Graziano Tassinato:** Funding acquisition. **Cristina Cavinato:** Writing – review & editing, Supervision, Resources, Project administration.

Funding

This study has been supported by ASI (Agenzia Spaziale Italiana) N. 2024–3-E.0 project “BioMOON – Low Gravity Biorefinery Platform” – Codice Unico di Progetto (CUP) F73D24000020001.

Declaration of competing interest

The authors declare that they have no known competing financial interests or personal relationships that could have appeared to influence the work reported in this paper.

Acknowledgments

This work was supported by the DoE 2023-2027 (MUR-Ministero dell’Universit à e della Ricerca (Italy), AIS.DIP.ECCELLENZA2023_27.FF project). The author sincerely thanks Alexandru Dron, from the University of Ca’ Foscari, for his kindly support with the SEM analysis.

Appendix A. Supplementary data

Supplementary data to this article can be found online at https://doi.org/10.1016/j.biortech.2025.133522.

Data availability

Data will be made available on request.

References

Aguirre Calvo, T., Santagapita, P., 2016. Physicochemical characterization of alginate beads containing sugars and biopolymers. J. Qual, Reliab. Eng. 2016, 9184039. Doi: 10.1155/2016/9184039.

Andreeva, A., Budenkova, E., Babich, O., Sukhikh, S., Ulrikh, E., Ivanova, S., Prosekov, A., Dolganyuk, V., 2021. Production, purification, and study of the amino acid composition of microalgae proteins. Molecules 26, 2767. https://doi.org/10.3390/molecules26092767.

Bajpai, S.K., Sharma, S., 2004. Investigation of swelling/degradation behaviour of alginate beads crosslinked with Ca^{2+} and Ba^{2+} ions. React. Funct. Polym. 59, 129–140. https://doi.org/10.1016/j.reactfunctpolym.2004.01.002.

Baldo, M.A., Fabris, S., Stortini, A.M., Daniele, S., 2024. Protolysis studies and quantification of acids and bases in aqueous solutions by microelectrode voltammetry. J. Solid State Electrochem. 28, 1049–1068. https://doi.org/10.1007/s10008-023-05675-8.

Banerjee, S., Tiwade, P.B., Sambhav, K., Banerjee, C., Bhaumik, S.K., 2019. Effect of alginate concentration in wastewater nutrient removal using alginate-immobilized microalgae beads: Uptake kinetics and adsorption studies. Biochem. Eng. J. 149, 107241. https://doi.org/10.1016/j.bej.2019.107241.

Barcellos, B. S. de C., Gutterres, M., 2024. Growth of *Chlorella vulgaris* during active immobilisation in calcium alginate. Appl. Biochem. Microbiol. 60, 1187–1195. Doi: 10.1134/S0003683823603062.

Bauer, L.M., Rodrigues, E., Rech, R., 2020. Potential of immobilized *Chlorella minutissima* for the production of biomass, proteins, carotenoids and fatty acids. Biocatal. Agric. Biotechnol. 25, 101601. https://doi.org/10.1016/j.bcab.2020.101601.

Benasla, A., Hausler, R., 2018. Optimisation of growth of *Raphidocelis subcapitata* immobilised for biofuel production: Influence of alginate and $CaCl_2$ concentrations on growth. Environ. 5, 60. https://doi.org/10.3390/environments5050060.

Canelli, G., Murciano Martínez, P., Maude Hauser, B., Kuster, I., Rohfritsch, Z., Dionisi, F., Bolten, C.J., Neutsch, L., Mathys, A., 2021. Tailored enzymatic treatment of *Chlorella vulgaris* cell wall leads to effective disruption while preserving oxidative stability. LWT 143, 111157. https://doi.org/10.1016/j.lwt.2021.111157.

Cao, S., Teng, F., Wang, T., Li, X., Lv, J., Cai, Z., Tao, Y., 2020. Characteristics of an immobilized microalgae membrane bioreactor (iMBR): Nutrient removal, microalgae growth, and membrane fouling under continuous operation. Algal Res. 51, 102072. https://doi.org/10.1016/j.algal.2020.102072.

Ciarleglio, G., Cinti, F., Toto, E., Santonicola, M.G., 2023. Synthesis and characterization of alginate gel beads with embedded zeolite structures as carriers of hydrophobic curcumin. Gels 9, 714. https://doi.org/10.3390/gels9090714.

Cycil, L.M., Hausrath, E.M., Ming, D.W., Adcock, C.T., Raymond, J., Remias, D., Ruemmele, W.P., 2021. Investigating the growth of algae under low atmospheric pressures for potential food and oxygen production on Mars. Front. Microbiol. 12, 733244. https://doi.org/10.3389/fmicb.2021.733244.

de Jesus, G.C., Gaspar Bastos, R., Altenhofen da Silva, M., 2019. Production and characterization of alginate beads for growth of immobilized *Desmodesmus subspicatus* and its potential to remove potassium, carbon and nitrogen from sugarcane vinasse. Biocatal. Agric. Biotech. 22, 101438. https://doi.org/10.1016/j.bcab.2019.101438.

De Micco, V., Amitrano, C., Mastroleo, F., Aronne, G., Battistelli, A., Carnero-Diaz, E., De Pascale, S., Detrell, G., Dussap, C.G., Ganigué, R., Jakobsen, Ø.M., Poulet, L., Van Houdt, R., Verseux, C., Vlaeminck, S.E., Willaert, R., Leys, N., 2023. Plant and microbial science and technology as cornerstones to Bioregenerative Life support Systems in space. npj Microgravity 9, 69. https://doi.org/10.1038/s41526-023-00317-9.

Fahrion, J., Mastroleo, F., Dussap, C.G., Leys, N., 2021. Use of photobioreactors in regenerative life support systems for human space exploration. Front. Microbiol. 12, 699525. https://doi.org/10.3389/fmicb.2021.699525.

Fuad, M.T.K., Khalid, A.A.H., Kamarudin, K.F., 2021. Sustainable cultivation of *Desmodesmus armatus* SAG276.4d using leachate as a growth supplement for simultaneous biomass production and CO_2 fixation. Int. J. Renew. Energy Dev. 10, 865–873. https://doi.org/10.14710/IJRED.2021.37683.

Gomez, C.G., Pérez Lambrecht, M.V., Lozano, J.E., Rinaudo, M., Villar, M.A., 2009. Influence of the extraction-purification conditions on final properties of alginates obtained from brown algae (*Macrocystis pyrifera*). Int. J. Bio. Macromol. 44, 365–371. https://doi.org/10.1016/j.ijbiomac.2009.02.005.

Griffiths, M.J., Garcin, C., van Hille, R.P., Harrison, S.T.L., 2011. Interference by pigment in the estimation of microalgal biomass concentration by optical density. J. Microbiol. Methods 85, 119–123. https://doi.org/10.1016/j.mimet.2011.02.005.

Han, M., Zhang, C., Ho, S.H., 2023. Immobilized microalgal system: an achievable idea for upgrading current microalgal wastewater treatment. ESE 14, 100227. https://doi.org/10.1016/j.ese.2022.100227.

Hu, X., Meneses, Y.E., Hassan, A.A., Stratton, J., Huo, S., 2021. Application of alginate immobilized microalgae in treating real food industrial wastewater and design of annular photobioreactor: a proof-of-concept study. Algal Res. 60, 102524. https://doi.org/10.1016/j.algal.2021.102524.

Kashima, K., Imai, M., 2012. Impact factors to regulate mass transfer characteristics of stable alginate membrane performed superior sensitivity on various organic chemicals. Procedia Eng. 42, 964–977. https://doi.org/10.1016/j.proeng.2012.07.490.

Kashima, K., Imai, M., 2017. Selective diffusion of glucose, maltose, and raffinose through calcium alginate membranes characterized by a mass fraction of guluronate. FBP 102, 213–221. https://doi.org/10.1016/j.fbp.2016.11.003.

Klopotic, J., Wyman, D., Petrie, Z., Wetzel, J., 2023. 52nd International Conference on Environmental Systems Design of a Trash Compaction & Processing System (TCPS). For Waste Management and Logistics Reduction in Long Duration Spaceflight.

Lacroux, J., Seira, J., Trably, E., Bernet, N., Steyer, J.P., van Lis, R., 2021. Mixotrophic growth of Chlorella sorokiniana on Acetate and Butyrate: Interplay between Substrate, C:N Ratio and pH. Front. Microbiol. 12, 703614. https://doi.org/10.3389/fmicb.2021.703614.

Lee, B.B., Ravindra, P., Chan, E.S., 2013. Size and shape of calcium alginate beads produced by extrusion dripping. Chem. Eng. Technol. 36, 1627–1642. https://doi.org/10.1002/ceat.201300230.

Liu, H., Yu, S., Liu, B., Xiang, S., Jiang, M., Yang, F., Tan, W., Zhou, J., Xiao, M., Li, X., Richardson, J.J., Lin, W., Zhou, J., 2024. Space-efficient 3D microalgae farming with optimized resource utilization for regenerative food. Adv. Mater. 36, 4011722. https://doi.org/10.1002/adma.2024011722.

Malektaj, H., Drozdov, A.D., deClaville Christiansen, J., 2023. Swelling of homogeneous alginate gels with multi-stimuli sensitivity. Int. J. Mol. Sci. 24, 5064. https://doi.org/10.3390/ijms24065064.

Masoomi Dezfooli, S., Bonnot, C., Gutierrez-Maddox, N., Alfaro, A.C., Seyfoddin, A., 2022. Chitosan coated alginate beads as probiotic delivery system for New Zealand black footed abalone (*Haliotis iris*). J. App. Pol. Sci. 139, 52626. https://doi.org/10.1002/app.52626.

Matyash, M., Despang, F., Ikonomidou, C., Gelinsky, M., 2014. Swelling and mechanical properties of alginate hydrogels with respect to promotion of neural growth. Tissue Eng. Part C 20, 401–411. https://doi.org/10.1089/ten.tec.2013.0252.

Mendes, A.R., Spínola, M.P., Lordelo, M., Prates, J.A.M., 2024. Chemical compounds, bioactivities, and applications of *Chlorella vulgaris* in food, feed and medicine. App. Sci. 14, 10810. https://doi.org/10.3390/app142310810.

Moreno-Garrido, I., 2008. Microalgae immobilization: current techniques and uses. Biores. Technol. 99, 3949–3964. https://doi.org/10.1016/j.biortech.2007.05.040.

Murujew, O., Whitton, R., Kube, M., Fan, L., Roddick, F., Jefferson, B., Pidou, M., 2021. Recovery and reuse of alginate in an immobilized algae reactor. Environ. Technol. 42, 1521–1530. https://doi.org/10.1080/09593330.2019.1673827.

Naskar, P., Chakraborty, D., Mondal, A., Das, B., Samanta, A., 2024. Immobilization of α-amylase in calcium alginate-gum odina (CA-GO) beads: an easily recoverable and reusable support. Int. J. Biol. Macromol. 258, 129062. https://doi.org/10.1016/j.ijbiomac.2023.129062.

Neves, B.S., Gonçalves, R.C., Mano, J.F., Oliveira, M.B., 2024. Controlling the diffusion of small molecules from matrices processed by all-aqueous methodologies: towards the development of green pharmaceutical products. Green Chem. 26, 4417–4431. https://doi.org/10.1039/d3gc04183b.

Pastore, M., Santaeufemia, S., Bertucco, A., Sforza, E., 2018. Light intensity affects the mixotrophic carbon exploitation in *Chlorella protothecoides*: Consequences on microalgae-bacteria based wastewater treatment. Water Sci. Technol. 78, 1762–1771. https://doi.org/10.2166/wst.2018.462.

Privman, V., Domanskyi, S., Luz, R.A.S., Guz, N., Glasser, M.L., Katz, E., 2016. Diffusion of oligonucleotides from within iron-cross-linked, polyelectrolyte-modified alginate beads: a model system for drug release. ChemPhysChem 17, 976–984. https://doi.org/10.1002/cphc.201501186.

Procházková, G., Šafařík, I., Brányik, T., 2012. Surface modification of *Chlorella vulgaris* cells using magnetite particles. Procedia Eng. 42, 1778–1787. https://doi.org/10.1016/j.proeng.2012.07.572.

Revellame, E.D., Aguda, R., Gatdula, K.M., Holmes, W., Fortela, D.L., Sharp, W., Gang, D., Chistoserdov, A., Hernandez, R., Zappi, M.E., 2024. Microalgae in bioregenerative life support systems for space applications. Algal Res. 77, 103332. https://doi.org/10.1016/j.algal.2023.103332.

Rungsima, C., Boonyan, N., Klorvan, M., Kusuktham, B., 2021. Hydrogel sensors with pH sensitivity. Polym. Bull. 78, 5769–5787. https://doi.org/10.1007/s00289-020-03398-8.

Santomartino, R., Averesch, N.J.H., Bhuiyan, M., Cockell, C.S., Colangelo, J., Gumulya, Y., Lehner, B., Lopez-Ayala, I., McMahon, S., Mohanty, A., Santa Maria, S. R., Urbaniak, C., Volger, R., Yang, J., Zea, L., 2023. Toward sustainable space exploration: a roadmap for harnessing the power of microorganisms. Nat. Commun. 14, 1. https://doi.org/10.1038/s41467-023-37070-2.

Smith, A., Bullard, T., Seatta, D., Hoque, B., Devito, C., Haarmann, K., Bair, R., Yeh, D., Long, P., Fehrenbach, M., Fischer, J., Roberson, L., 2022. Management of fecal waste utilizing a hybrid organic processor assembly unit designed for resource recovery. https://hdl.handle.net/2346/89788.

Souza, M.D.P., Brasil, S.L.D.C., Melo, R.S., Zanardi, C., Daniele, S., 2024. Voltammetry of the ferric/ferrous redox couple at platinum microelectrodes in aqueous hydrochloric acid. J. Electroanal. Chem. 969, 118543. https://doi.org/10.1016/j.jelechem.2024.118543.

Spínola, M.P., Costa, M.M., Prates, J.A.M., 2023. Enhancing digestibility of *Chlorella vulgaris* biomass in monogastric diets: strategies and insights. Animals 13, 1017. https://doi.org/10.3390/ani13061017.

Stefan-Kharicha, M., Kharicha, A., Mogeritsch, J., Wu, M., Ludwig, A., 2018. Review of ammonium chloride-water solution properties. J. Chem. Eng. Data 63, 3170–3183. https://doi.org/10.1021/acs.jced.7b01062.

Tam, N.F.Y., Wong, Y.S., 2000. Effect of immobilized microalgal bead concentrations on wastewater nutrient removal. Environ Pollut. 107, 145–151. https://doi.org/10.1016/S0269-7491(99)00118-9.

Vetrano, A., Gabriele, F., Spreti, N., 2023. Prevention of Swelling Phenomenon of Alginate Beads to Improve the Stability and Recyclability of Encapsulated Horse Liver Alcohol Dehydrogenase. ChemBioChem 24, 300456. https://doi.org/10.1002/cbic.202300456.

Volpin, F., Badeti, U., Wang, C., Jiang, J., Vogel, J., Freguia, S., Fam, D., Cho, J., Phuntsho, S., Shon, H.K., 2020. Urine treatment on the international space station: current practice and novel approaches. Membranes 10, 327. https://doi.org/10.3390/membranes10110327.

Wang, Y., Ma, J., Chu, H., Zhou, X., Zhang, Y., 2024. Advances in microalgae-based livestock wastewater treatment: Mechanisms of pollutants removal, effects of inhibitory components and enhancement strategies. Chem. Eng. J. 483, 149222. https://doi.org/10.1016/j.cej.2024.149222.

Yoshida, K., Kashima, K., 2025. Nano-structural modification of mass transfer channels in alginate membrane by dispersed oligoethylene glycol for nanofiltration applications. Colloid Polym. Sci. 303, 1261–1271. https://doi.org/10.1007/s00396-025-05408-5.

Zazzali, I., Aguirre Calvo, T.R., Pizones Ruíz-Henestrosa, V.M., Santagapita, P.R., Perullini, M., 2019. Effects of pH, extrusion tip size and storage protocol on the structural properties of Ca(II)-alginate beads. Carbohydr. Polym. 206, 749–756. https://doi.org/10.1016/j.carbpol.2018.11.051.